THE ASTROPHYSICAL JOURNAL, 464:704–714, 1996 June 20

HUBBLE SPACE TELESCOPE ULTRAVIOLET SPECTRUM OF ARP 102B, THE PROTOTYPICAL DOUBLE-PEAKED EMISSION-LINE AGN

JULES P. HALPERN
Columbia Astrophysics Laboratory, Columbia University, 538 West 120th Street, New York, NY 10027
MICHAEL ERACLEOUS[1]
Space Telescope Science Institute, 3700 San Martin Drive, Baltimore, MD 21218
ALEXEI V. FILIPPENKO
Department of Astronomy, University of California, Berkeley, CA 94720
AND
KAIYOU CHEN
Los Alamos National Laboratory, Theoretical Division, T-6, Los Alamos, NM 87545
Received 1995 September 29; accepted 1996 January 8

ABSTRACT

UV spectra of the nucleus of the elliptical galaxy Arp 102B were obtained with the *HST*'s Faint Object Spectrograph in order to investigate the UV emission-line counterparts of its unusual double-peaked Balmer lines. Broad Mg II λ2798 is present with nearly the same profile as the Balmer lines (peaks separated by $\approx$12,000 km s^{-1}), and a typical Mg II/Hβ ratio of 1. But there is little, if any C III] λ1909 or C IV λ1550 emission corresponding to the displaced Balmer-line peaks. Most important, there is no double-peaked component detected in Lyα; the Lyα/Hβ ratio is less than 0.12 in the displaced peaks. However, there is an "ordinary," nondisplaced broad-line component with FWHM $\approx$ 3500 km s^{-1} in *all* of the permitted lines, demonstrating the need to invoke different locations and different physical conditions for double-peaked and single-peaked line components in the same object. The striking absence of displaced peaks in Lyα probably cannot be explained solely by reddening. Rather, it indicates that high density and large optical depth in Lyα are required to destroy the line photons by collisional de-excitation and possibly by bound-free absorption out of the $n = 2$ level of hydrogen. These results strongly support the application, at least to Arp 102B, of the accretion-disk model of Dumont & Collin-Souffrin, in which the disk produces only low-ionization lines and a Lyα/Hβ ratio that agrees with our observed upper limit.

Also present is an extraordinary system of absorption lines at the systemic redshift of Arp 102B, in which metastable levels of Fe II up to 1.1 eV above the ground state participate in addition to the more common resonance transitions. Absorption from metastable levels of Fe II have been seen previously only in two unusual, low-ionization broad absorption-line QSOs, Q0059 – 2735 and Mrk 231. Temperatures and densities needed to excite these levels are similar to narrow-line region conditions. Why they are seen in absorption in Arp 102B, a relatively unobscured active galactic nucleus, but in no other Seyfert or radio galaxy, is a mystery.

Subject headings: accretion, accretion disks — galaxies: active — galaxies: individual (Arp 102B) — galaxies: nuclei — line: profiles — quasars: absorption lines

1. INTRODUCTION

The broad-line radio galaxy Arp 102B (Biermann et al. 1981; Stauffer, Schild, & Keel 1983; Puschell et al. 1986) was proposed as the prototypical accretion-disk emitter among active galactic nuclei (AGNs) because of the resemblance of its extremely broad, double-peaked Balmer line profiles to the results of a simple kinematic model of an accretion disk (Chen, Halpern, & Filippenko 1989; Chen & Halpern 1989). Tests of this and other hypotheses have proceeded along a number of lines, including studies of the variability of its line profile (Halpern & Filippenko 1988, 1992; Eracleous & Halpern 1993; Miller & Peterson 1990), spectropolarimetry (Chen & Halpern 1990; Antonucci, Hurt, & Agol 1996), and spectroscopy of related objects (Halpern 1990; Veilleux & Zheng 1991; Zheng, Veilleux, & Grandi 1991; Eracleous & Halpern 1994; Halpern & Eracleous 1994; Sulentic et al. 1995; Storchi-Bergmann et al. 1995).

Previous ultraviolet observations of Arp 102B and other double-peaked emitters with the *International Ultraviolet Explorer* (*IUE*) were not of sufficiently high quality to reveal detailed information about their line profiles. As long as double peaks were detected only in Balmer lines, useful model predictions of line intensity ratios involving species of different ionization and excitation potential could not be tested. However, the *IUE* spectrum of Arp 102B presented by Chen et al. (1989) did show that Lyα, the only emission line detected, was narrower than the Balmer lines and had no evidence for emission at the velocities corresponding to the displaced Balmer-line peaks. Chen et al. placed an upper limit of 1 on the Lyα/Hβ ratio at the velocity of the displaced peaks and speculated that the cause was large optical depth in the line-emitting accretion disk. The absence of a UV bump was attributed to inflation of the inner disk into an optically thin ion-supported torus (Rees et al. 1982), which could also be the agent responsible for

[1] Hubble Fellow. Current address: Department of Astronomy, University of California, Berkeley, CA 94720.

illuminating the thin outer disk with hard, photoionizing radiation.

In this paper, we present the first *Hubble Space Telescope* (*HST*) ultraviolet spectrum of a double-peaked emitter, Arp 102B, which affords a more comprehensive means of evaluating the accretion-disk model through the intercomparison of a number of emission lines. Detailed theoretical predictions of emission lines from accretion disks were made in a series of papers by Collin-Souffrin (1987), Collin-Souffrin & Dumont (1990), and Dumont & Collin-Souffrin (1990a, b, c). The principal feature of the model is the illumination of a geometrically thin accretion disk by an external hard photoionizing source, either pointlike or diffuse, The main result which distinguishes this calculation from photoionization models of ordinary broad-line clouds is the weakness of the high-ionization lines, because the outer disk is assumed not to see the "UV bump" emission coming from the inner disk. Consequently, the high-ionization zone on the surface of the disk is relatively thin. In addition, the predicted Lyα line is weak because it is collisionally deexcited at high density. The Lyα/Hβ intensity ratio is less than 1 in many of the model runs. Both single-peaked and double-peaked lines can be produced, depending on the radial extent of the line-emitting disk. Detailed fits to the continuum and emission lines of several AGNs, including Arp 102B, were made by Rokaki, Boisson, & Collin-Souffrin (1992) using this model.

The *HST* spectra of Arp 102B cover all the UV emission lines from Lyα through Mg II λ2798. We also obtained nearly contemporaneous ground-based optical spectroscopy. The observations and basic data reductions are described in § 2. The measured properties of the emission lines are presented in § 3. Interpretation of the emission-line results in terms of accretion-disk and other models is discussed in § 4. In § 5, an unusual system of associated absorption lines is described. Our conclusions, and speculations about additional aspects of this subject, comprise § 6.

2. OBSERVATIONS AND BASIC DATA REDUCTION

2.1. *Ultraviolet Spectroscopy with the HST*

Ultraviolet spectra of Arp 102B were obtained with the *HST*'s Faint Object Spectrograph (FOS) through a circular aperture of diameter 0.″9 in a series of 11 exposures on 1994 November 18–20, after correction of the spherically aberrated optics. Three different gratings were used to cover the wavelength range 1153–3277 Å. A summary of the instrumental configuration, along with exposure time and spectral resolution, is given in Table 1. The reduction of the FOS data consisted of particle background subtraction, flat-field correction, and flux and wavelength calibration. The observed UV spectra themselves are shown in Figure 1, where the identified emission lines are marked. In this paper, we concentrate on the properties of the emission lines and the absorption lines. Although the FOS spectra are given in vacuum wavelengths, we will follow standard practice and quote air wavelengths when referring to lines longward of 2000 Å. The heliocentric correction for this observation is less than 5 km s^{-1} and has been neglected. Considering all sources of error, of which repeatability of the positioning of the grating wheel is the dominant effect, the net uncertainly in the wavelength scale corresponds to $\sim$80 km s^{-1} (Kriss, Blair, & Davidsen 1991a, b; Dahlem & Koratkar 1994; Koratkar & Evans 1995).

Spectra obtained with the FOS are sometimes contaminated by undispersed light from the zeroth order of the grating (and, to a lesser extent, dispersed light from higher orders) illuminating the parts of the detector array which record the first-order, dispersed light. This is known as the "scattered-light problem," and its effects are most significant in the spectra of red objects (Kinney & Bohlin 1993; Ayres 1993; Rosa 1993). To assess the level of scattered-light contamination of our own spectra we simulated the total distribution of counts from orders 0 to 5 on the detector array, using the software of Rosa (1994). The input to the simulation program is the observed spectrum of Arp 102B from 1150 to 8000 Å, which is the combination of the FOS spectra presented here and the optical spectra discussed below. The results of the simulation show that the scattered light contamination is negligible, of order 1% of the observed flux, for wavelengths longer than 1170 Å. Below 1170 Å the effect of scattered light becomes significant and is responsible for part of the upturn of the continuum seen at the shortest wavelengths of the G130H spectrum. The remainder of the upturn is probably particle-induced background.

2.2. *Optical Spectroscopy from the Ground*

The *HST* observations of Arp 102B were complemented by optical observations carried out at Lick Observatory. CCD spectra were obtained on three separate occasions with the Kast double spectrograph (Miller & Stone 1993) at the Cassegrain focus of the 3 m Shane reflector. A log of the observations, including exposure times and spectral coverage, is given in Table 2. A resolution of 6–8 Å was achieved with the 2″ slit. Conditions were generally clear during the observations, but the seeing was mediocre (typically 2.″5). To minimize the effects of atmospheric dispersion at the moderately high air masses (1.3–1.8), the slit was oriented along the parallactic angle, close to 80° in most cases. Thus the relative flux calibration should be accurate. Absolute fluxes are judged to be good to $\pm$20%–30%, but depend on

TABLE 1

HST OBSERVATIONS (1994 NOVEMBER 18–20 UT)

Detector-Grating Combination	Spectral Range (Å)	Spectral Resolution (Å)	Exposure Time (s)
Blue/G130H.....	1153–1606	0.98	13870
Blue/G190H.....	1573–2330	1.49	5880
Red/G270H	2222–3277	2.05	1980

TABLE 2

LICK OBSERVATIONS

UT Date (1994)	Spectral Range[a] (Å)	Exposure Time (s)
Aug 4	3240–5200, 5900–8040	1800
	4300–7000	1800
Sep 3.....	3240–5200, 5900–8040	1800
	4300–7000	1800
Nov 12.....	3240–5200, 5900–8040	1800
	4300–7000	1800
	3240–5200, 7900–9900	1000

[a] Each entry corresponds to a separate exposure. Up to two separate spectral regions can be observed simultaneously in the same exposure.

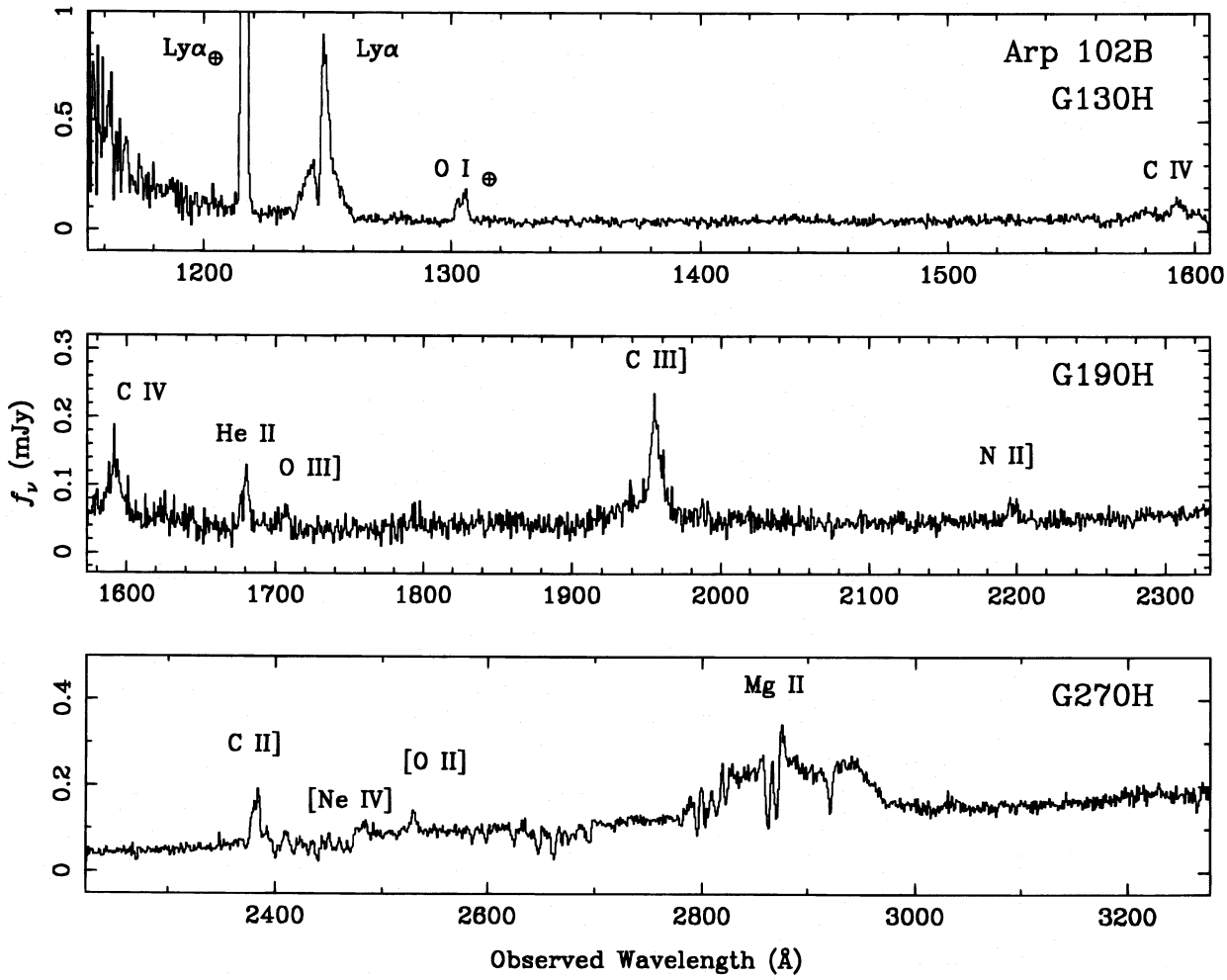

FIG. 1.—The *HST*/FOS spectra of Arp 102B. Each panel shows the spectrum from a different grating, in order of increasing wavelength. The spectra are binned with two bins per resolution element. Identifications of the most prominent emission lines are given.

the stability of the seeing during the course of the observations of the object and the standard stars.

Routine procedures were followed during reductions (e.g., Filippenko & Sargent 1988, and references therein). Spectra of Arp 102B and of standard stars observed in the same way were extracted from a 4″ window along the slit. This ensured that the flux calibration would be more accurate for spatially unresolved sources of radiation (the nonstellar continuum and broad emission lines) than for the extended sources (narrow emission lines and especially starlight). Telluric absorption lines were removed through division by the spectra of standard stars, which are intrinsically featureless in the relevant regions. In Figure 2 we show as an example the spectrum obtained on 1994 August 4 UT. There are no discernible differences between this spectrum and those obtained on the other two dates.

2.3. *Continuum Decomposition*

The ground-based optical spectrum of Arp 102B contains a substantial amount of starlight, which can affect the measurement of weak emission lines. In order to remove the stellar light, we modeled the continuum in the Lick spectrum as the sum of a power law plus a stellar template consisting of a spectrum of an elliptical galaxy. After experimenting with the spectra of several elliptical and S0 galaxies (NGC 3379, NGC 4339, NGC 4365, IC 4889) suitably corrected for Galactic extinction, as well as the composite giant elliptical galaxy spectrum of Yee & Oke (1978), we finally adopted NGC 4365 as the best starlight template. We adopted a Galactic extinction to Arp 102B of $E(B-V) = 0.045$ mag, corresponding to the 21 cm neutral hydrogen column of 2.3×10^{20} cm^{-2} along this line of sight (Stark et al. 1992). The parameters of the best-fitted decomposition are power-law index $\alpha = 2.1 \pm 0.3$ where $f_\nu \propto \nu^{-\alpha}$, and $f_\nu = 0.30 \pm 0.02$ mJy at a fiducial wavelength of $\lambda_{obs} = 3200$ Å. The fractional contribution of starlight is 0.22 ± 0.05 at rest wavelength 3600 Å (below the Ca II H and K break), and 0.38 ± 0.08 at 4300 Å (above the break). The error bars correspond to the dispersion in the continuum parameters derived from fits with different starlight templates. The following results indicate that the decomposition scheme is quite robust:

1. The continuum shape is reproduced almost perfectly, including the numerous stellar absorption lines (e.g., TiO, Na I D, Mg I b, Ca II H and K).
2. The dispersion in the continuum parameters derived from fits with different starlight templates is small.
3. Fits to only the red part of the spectrum (longward of 4600 Å) can reproduce the blue spectrum successfully when they are extrapolated to 3200 Å.

The FOS spectrum by itself is fitted by a power law of $\alpha = 2.4, f_\nu = 0.22$ mJy at $\lambda_{obs} = 3200$ Å, with some evidence

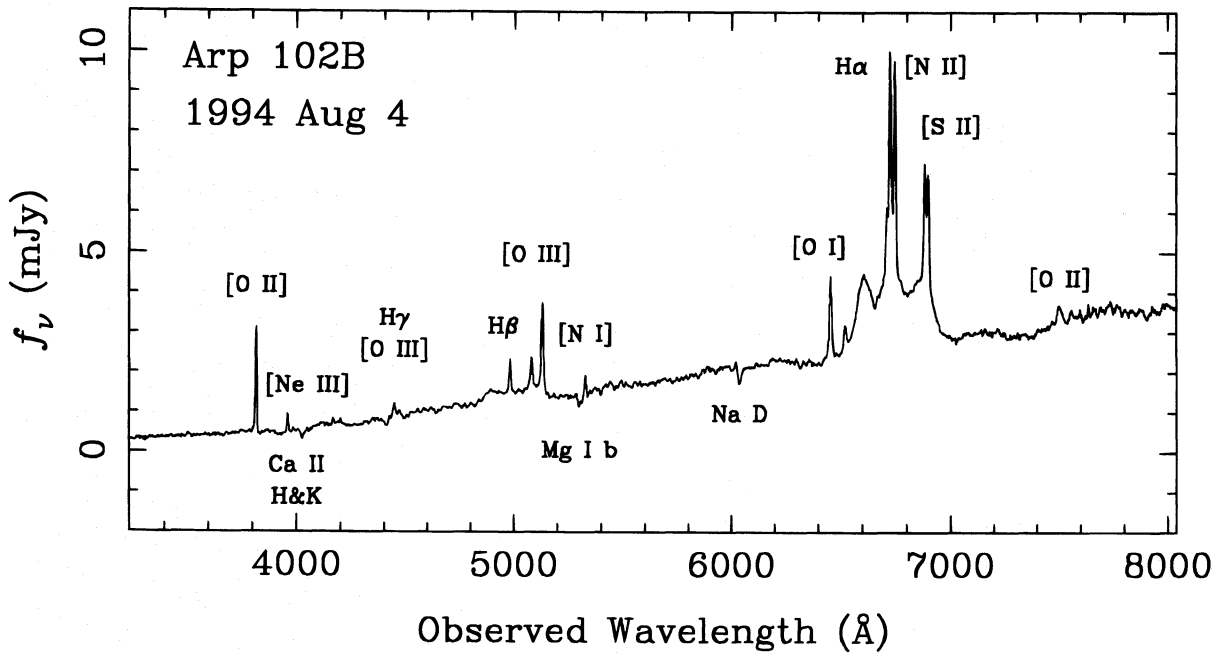

FIG. 2.—An example of the optical spectrum of Arp 102B, taken on 1994 Aug. 4, with the Lick 3 m telescope. The most prominent narrow emission lines are identified. Residual fringing in the CCD is visible redward of 7500 Å.

for an upturn below 1600 Å, which may be particle-induced background. There is no evidence for starlight in the FOS spectrum, consistent with its small aperture and an extrapolation of the decomposition of the Lick spectrum. Attempts to fit the FOS spectrum of Arp 102B with a model including FOS spectra of the elliptical galaxies NGC 1399 and NGC 3610, kindly made available by Henry Ferguson, yielded only upper limits of order 0.1 on the starlight fraction at $\lambda_{obs} = 3200$ Å.

These steep fitted power laws cannot extend into the near-infrared because they would exceed the observed fluxes at 3.5 and 10 μm (Puschell et al. 1986). A power law connecting the observed 10 μm point to the 3200 Å flux would be much flatter, with $\alpha = 1.3$. The latter value is much closer to the overall spectral index that would describe the broadband continuum from 60 μm through X-rays (see Fig. 7 of Chen et al. 1989). We will address continuum issues more completely in a later paper.

3. EMISSION LINES

The major emission lines were measured from the FOS and Lick spectra, the latter after the removal of the stellar and nonstellar continuum as described above. Since there is no evidence for a significant starlight continuum component in the FOS spectra, a power law or polynomial was used to model the continuum around each line. The results are listed in Table 3, where both observed and dereddened fluxes are given. The presence of narrow absorption lines at the systemic velocity superposed on all of the UV resonance lines renders the measurement of the narrow-line region component highly inaccurate, so we discuss only their broad components here.

In the case of the Balmer lines, the peculiar profiles were decomposed into three components representing (1) a disklike profile with model parameters nearly identical to those fitted by Chen & Halpern (1989), (2) a broad Gaussian at zero velocity, with FWHM $\approx$ 3500 km s^{-1}, that remains after removal of the disklike component, and (3) a narrow-line contribution that remains after the broad Gaussian is removed. Although this is obviously a model-dependent measurement procedure, it is well justified by the ease with which the components are distinguished, and by the considerable insight that ensues when the results are compared with those of the UV lines. A comparison of the major broad emission-line profiles is given in Figure 3, after continuum subtraction, together with fits of a disklike profile to those lines which clearly possess such a component. The parameters of the fits are given in the footnote to Table 3.

Of all the lines in the ultraviolet, Mg II is the only one that shows a clear disklike profile. Despite the forest of absorption lines that blanket it, a disk model with parameters very similar to that of the Balmer lines fits the envelope of Mg II quite well. The disklike profile superposed on the Mg II line in Figure 3 is *not* the best-fitted model, but rather a doublet with exactly the same parameters that fitted the Balmer lines. This illustrates that the Mg II line is slightly but significantly broader than the Balmer lines. A model that is optimized to fit the Mg II line corresponds instead to a disk that is $\sim$10% smaller than the one illustrated. Subtraction of an optimal disklike model from Mg II leaves a broad residual at zero velocity that can be fitted by a Gaussian of FWHM $\approx$ 3800 km s^{-1}, also very similar to that of the Balmer lines.

The C IV line is very weak, with a core of FWHM $\approx$ 4700 km s^{-1}, and only a hint of displaced peaks that would correspond to the disklike component. Fitting of this line is hampered by its truncation at the ends of both the G130H and G190H spectra. Nevertheless, we have been able to assign a very uncertain disklike contribution to C IV (see Fig. 3) with the same parameters as those of the Balmer lines, and a ratio C IV/Hβ = 0.19 in this component. There are possibly also broad absorption features in C IV extending to -5000 km s^{-1}. Although these features in the C IV line could be very important, we will not discuss them

TABLE 3

EMISSION-LINE MEASUREMENTS OF ARP 102B

Line Identification	Flux[a] $F/F(\mathrm{H}\beta[n])$	Intensity[b] $I/I(\mathrm{H}\beta[n])$	FWHM (km s^{-1})	Comment
Lyα[narrow]	2.13	2.73	630	Affected by absorption
Lyα[broad]	6.69	8.60	3240	
Lyα[disklike]	<0.67	<0.86	...	Disk-model fit[c]
C IV λ1550[n]	0.07	0.08	900	Affected by absorption
C IV λ1550[b]	1.28	1.53	4710	
C IV λ1550[d]	1.07	1.29	...	Disk-model fit[c]
He II λ1640	0.41	0.49	950	
O III] λ1663	0.12	0.14	1020	
C III] λ1909	0.99	1.21	1510	
C III] λ1909[d]	<0.29	<0.36	...	Disk-model fit[c]
N II] λ2141	0.10	0.12	1140	
C II] λ2326	0.40	0.49	1040	20% uncertainty
[Ne IV] λ2423	0.08	0.09	560	Interstellar Fe II abs.
[O II] λ2740	0.13	0.15	610	
Mg II λ2798[n]	...	...	...	Removed by absorption
Mg II λ2798[b]	0.77	0.84	3750	
Mg II λ2798[d]	5.12	5.64	...	Disk-model fit[c]
[O II] λ3727	4.10	4.27	500	
[Ne III] λ3869	0.67	0.70	470	
[Ne III] λ3968	0.14	0.15	360	
[S II] λ4068	0.21	0.22	315	
[S II] λ4076	0.03	0.03	340	
Hδ[n]	0.17	0.17	280	
Hγ[n]	0.54	0.55	800	
Hγ[d]	1.39	1.42	...	Disk-model fit[c]
[O III] λ4363	0.28	0.28	1290	Highly uncertain
Hβ[n]	1.00	1.00	530	
Hβ[b]	0.46	0.46	3530	Highly uncertain
Hβ[d]	5.67	5.67	...	Disk-model fit[c]
[O III] λ4959	0.86	0.86	620	
[O III] λ5007	2.62	2.61	610	
[N I] λ5199	0.38	0.38	370	
He I λ5876[n]	0.20	0.19	530	
[O I] λ6300	1.55	1.48	450	
[O I] λ6363	0.39	0.38	420	Highly uncertain
[N II] λ6548	1.05	1.00	430	
Hα[n]	3.47	3.31	400	
Hα[b]	5.45	5.19	3550	
Hα[d]	25.68	24.48	...	Disk-model fit[c]
[N II] λ6583	3.09	2.94	370	
[S II] λ6716	1.99	1.89	460	
[S II] λ6731	1.49	1.41	290	
[O II] λ7319	0.27	0.26	650	
[O II] λ7330	0.14	0.13	690	

[a] Observed flux relative to $F(\mathrm{H}\beta[n]) = 1.23 \times 10^{-14}$ ergs cm^{-2} s^{-1}.

[b] Intensity corrected for $E(B-V) = 0.045$ mag, relative to $I(\mathrm{H}\beta[n]) = 1.43 \times 10^{-14}$ ergs cm^{-2} s^{-1}.

[c] Model parameters are $r_1 = 330GM/c^2$, $r_2 = 970GM/c^2$, $q = 3$, $i = 32°$, $\sigma = 850$ km s^{-1}. Emissivity is proportional to r^{-q} between limits r_1 and r_2. Inclination angle i is between the axis of the disk and the line of sight. Additional broadening parameter σ is defined in Chen & Halpern 1989. Fits to the data are shown in Fig. 3.

further because they are too weak to characterize definitively.

The Lyα line is the most interesting for its striking absence of displaced double peaks. A fit of the disk model to the noise on either side of the line yields an upper limit which corresponds to Lyα/Hβ < 0.12 in this component. A Gaussian that fits the broad Lyα line has FWHM ≈ 3200 km s^{-1}, not significantly different from the same component in the Balmer lines of in Mg II. The Lyα/Hβ ratio in the Gaussian component is ∼10, more typical of Seyfert galaxies and quasars, as is the Lyα/C IV ratio of ∼5. The existence of this "ordinary" broad-line component in all of the permitted lines (except for He II in which this component may be too weak to detect) is the reason that we have confidence in the existence of two distinct sources of the broad lines in Arp 102B. In § 4, we consider and reject differential reddening of these two sources as a sufficient explanation for the absence of a double-peaked component of Lyα. Instead, we argue that one of the emission-line sources has properties consistent with standard broad-line clouds, while the other is in agreement with accretion disk models, and that neither is significantly reddened.

The semiforbidden lines of C III] λ1909, C II] λ2326, N II] λ2141, and O III] λ1663 all have widths of 1000–1500 km s^{-1}, broader than the forbidden lines, but narrower than the broad Gaussian components of the permitted lines. Therefore, they may arise in a continuum of emission-line clouds between these extremes. From the blue side of the C III] line, we deblended a possible weak line of Si III] λ1892 which contributes some residual uncertainty to the width

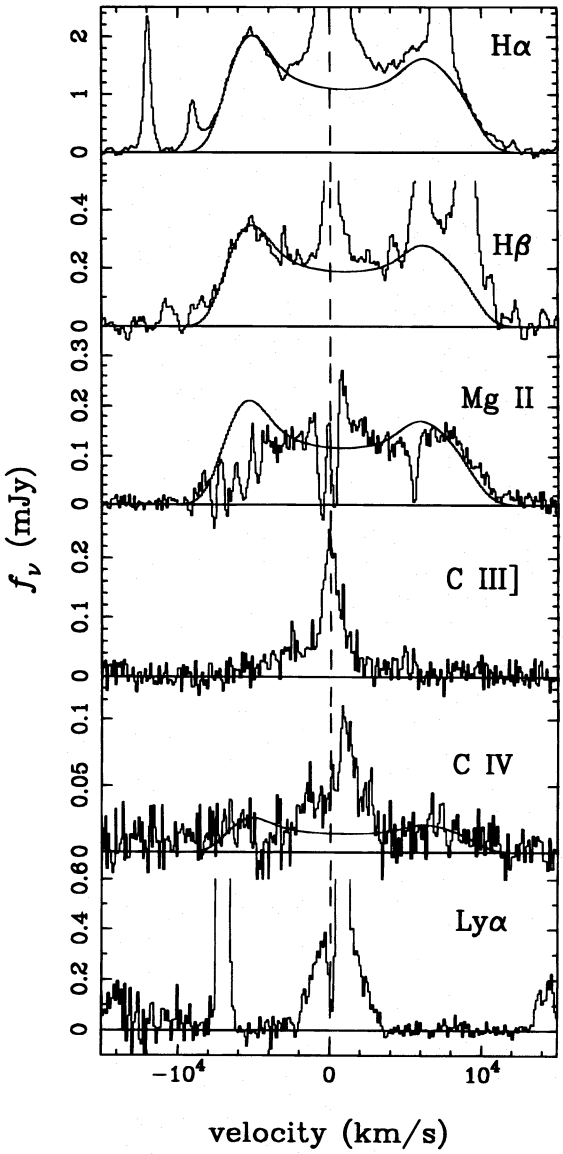

FIG. 3.—Comparison of emission-line profiles of Arp 102B. Zero velocity corresponds to the narrow emission-line redshift, $z = 0.02438$. The best-fitted disklike model for the Balmer lines is shown, and the same model is superposed on the Mg II and C IV profiles. The model parameters are given in the footnote to Table 3. The FOS spectra are binned with two bins per resolution element.

and strength of C III]. Also, the C II] line is probably underestimated in strength because it is contaminated by Fe II absorption.

4. INTERPRETATIONS OF THE DOUBLE-PEAKED EMISSION LINES

It is clear from the existence of both single-peaked and double-peaked emission lines that these are emitted in physically distinct locations. We do not restrict the meaning of "distinct locations" necessarily to different types of structures, such as disk and clouds. Different locations in an accretion disk or physically separated flows of clouds could be hypothesized. But since the single-peaked broad-line components are present in essentially normal ratios, we begin with the simple assumption that they represent a normal broad line region, possibly (but not necessarily) composed of standard broad-line clouds. We then proceed to evaluate a number of candidate explanations for the double-peaked lines, and for the absence of double-peaked Lyα.

4.1. *Evaluation of Extinction*

Whatever the source of the double-peaked Balmer lines, we first examine the hypothesis that the absence of double-peaked Lyα can be attributed to *external* reddening of that source. The observed intensity ratios of Hα, Hβ, and Mg II in their respective double-peaked components make this extremely unlikely. Consider the Hα/Hβ ratio of 4.3. If we assume that the intrinsic ratio after dereddening should not be less than 3.1, then $E(B-V) < 0.32$ mag. But dereddening by even this extreme value will only increase the upper limit on the *intrinsic* Lyα/Hβ ratio to 1.0, which is still several times less than the *observed* values in AGNs, which range from 2 to 10. Another indicator that reddening is not severe is the Mg II/Hβ ratio of 1.0, also a typical value. An assumed extinction of $E(B-V) = 0.6$ mag, which brings the intrinsic Lyα/Hβ ratio up to 5, would also increase the Mg II/Hβ ratio to 3.8, and decrease the Hα/Hβ ratio to 2.3, both outside the normal range. Of course, we base this analysis on the expected line ratios from recombination theory and AGN observations; it is possible that the intrinsic ratios in Arp 102B are quite different. But that only reinforces our point. External reddening of the source of the double-peaked lines is not a sufficient explanation of its peculiar line ratios, especially the severe upper limit on Lyα/Hβ.

Neither is it possible to invoke *differential* reddening of emitters distributed among absorbers to explain these line ratios. In this scenario, the redder lines should contain more flux from regions of higher extinction than the bluer lines. Therefore, the extinction measured from the Hα/Hβ ratio should be larger than that from the Lyα/Mg II ratio. Instead, the opposite is observed. Hα/Hβ indicates minimal reddening, and is in fact consistent with values observed in other AGNs and calculated in photoionization models of both clouds and disks.

It is possible, however, that a small amount of dust mixed *internally* with the emitting gas could efficiently remove Lyα because of its large optical depth to resonant scattering. This effect is similar to other processes that selectively remove Lyα, such as resonant absorption followed by collisional de-excitation, or bound-free absorption from neutral metals or the $n = 2$ level of hydrogen. To be effective, any of these processes would necessarily involve large Lyα optical depths *over the entire range of velocities covered by the double-peaked lines.* Such an absorber is therefore effectively cospatial with the emitter. Furthermore, the hypothesized absorbing/emitting structure must not obstruct our view of the source of the ordinary broad-line component observed in Lyα, and so must be smaller, and probably closer to the ionizing source, than the broad-line region. But it also must not shield the broad-line region from the ionizing continuum. An accretion disk is an obvious candidate for the structure that will satisfy all of these requirements.

The existence of dust within both clouds and accretion disks has long been considered a possibility, although extinction by dust is not thought to be the sole cause of the small Lyα/Hβ ratio even in normal quasars. The latest conclusion (of Netzer & Laor 1993) is that dust is unlikely to be present in broad-line region clouds that are responsible for

most of the observed line emission. Indeed, these authors propose that the outer boundary of the broad-line region is determined by the distance at which dust sublimes. Similarly, Collin-Souffrin & Dumont (1990) concluded that dust grains are destroyed in the radiatively heated surface of an accretion disk in the zone from which the line emission is hypothesized to originate. Although dust could be present in the inner layers of the disk, such a configuration would not contribute to extinction of the observed Lyα. In any case, since we are now considering internal reddening, any such hypothesized structure is identical with the emission-line region itself. Therefore, we proceed to evaluate models of emission-line sources that might accomplish the job of reproducing these extraordinary double-peaked line profiles and ratios.

4.2. *A Photoionized Accretion Disk*

Photoionization models of illuminated accretion disks were exhaustively treated in a series of papers by Collin-Souffrin & Dumont (1990) and Dumont & Collin-Souffrin (1990a, b, c). Specific application of those models to Arp 102B was made by Rokaki et al. (1992). We summarize here the fundamental properties of this disk model that explain why its results differ greatly from photoionization models of clouds. Most important is the high density of the disk. its density can exceed 10^{15} cm^{-3}, and its vertical column density in the region responsible for the Balmer lines is much greater than the $\sim 10^{25}$ cm^{-2} value past which ionizing radiation does not penetrate. The large hydrogen density is responsible for the trapping and collisional deexcitation of Lyα in the region of the disk in which Balmer lines are copiously produced. In contrast, even the newer photoionization models of high-density broad-line clouds (Rees, Netzer, & Ferland 1989), with densities as high as 10^{13} cm^{-3} and $N_{\rm H} = 10^{23}$ cm^{-2}, do not produce Lyα/Hβ ratios less than 10.

Also very important is the adopted ionizing spectrum, in which any "UV bump" is assumed not to be seen by the outer disk. Rather, the illuminating spectrum is a power law extending to 100 keV with a spectral index not steeper than 1, consistent with X-ray observations of Seyfert galaxies. The paucity of soft ionizing photons from a UV bump makes the high-ionization zone relatively thin. The bulk of the ionizing flux is deposited in a low-ionization region which produces mostly Balmer lines, Mg II, and Fe II emission.

Despite some uncertainty about the geometry and spectrum of the illuminating source, this model is a particularly attractive one for Arp 102B because, as originally pointed out by Chen et al. (1989), it is not seen to possess a UV bump. Therefore, speculation about whether or not that particular component comes from the inner disk, and whether or not it is seen by the outer disk, is moot. With only a hard, nonthermal continuum remaining, the emission-line ratios are insensitive to the luminosity, and only weakly dependent upon the geometry of illumination. Rokaki et al. (1992) were able to fit the broad-band continuum, emission-line fluxes, and emission-line ratios of Arp 102B with a model whose ionizing luminosity is consistent with an extrapolation of the *Einstein* X-ray flux (Biermann et al. 1981). Most remarkably, their computed Lyα/Hβ ratio is 0.15, which is exactly equal to our (dereddened) upper limit for the disklike component! They made this prediction without knowing what fraction of the Lyα line (poorly observed by *IUE*) should be attributed to the broad-line region. We now know that it is $\sim$70%, of which less than 10% is in a double-peaked component.

The results of this model, as far as it goes, are in excellent agreement with the data. An additional useful feature is the moderate optical depth in the Balmer continuum, which indicates that photoionization out of the $n = 2$ level may be an important suppressor of Lyα as pointed out by Shields & Ferland (1993). Mg II λ2798 can also ionize hydrogen out of $n = 2$, but its abundance makes its optical depth to resonance scattering much smaller, facilitating escape. Another conclusion of the Rokaki et al. model is that a diffuse ionizing source is required to fit the Balmer line profiles. A sphere of radius $r = 300GM/c^2$ was fitted by Rokaki et al., which is in excellent agreement with our analytic approximation (see the footnote to Table 3) in which the region of most intense line emission is at the fitted inner boundary of a thin disk at $r_1 = 330GM/c^2$. Numerically, this radius is in accord with our previous speculation that the ionizing source might in fact be the inner disk itself, inflated into an ion torus, with height $h \simeq r$ and radius r given by equation (13) of Chen & Halpern (1989). Further details of the Rokaki et al. model, such as the strength and profile of Mg II, were not published. It would be interesting, for example, to see if the model Mg II line is slightly wider than the Balmer lines, as figure 3 shows.

In summary, both the line ratios and profiles in Arp 102B have found a natural explanation in an illuminated accretion disk. In the remainder of this section, we evaluate some alternative models in the light of our new data.

4.3. *Alternative Models for Double-Peaked Emission Lines*

One of the oldest models for displaced or double-peaked emission lines in AGNs is the supermassive binary black hole, in which each has its own broad-line region (Gaskell 1983). Although this is still a viable explanation for peculiar line profiles in some AGNs, it was never an attractive one for objects like Arp 102B in which there are two relatively well separated peaks at high velocity. The actual line profile of such a binary should be more blended. The near symmetry of the peaks in Arp 102B would, additionally, require the coincidence of nearly identical masses, and the large velocities would require a short orbital period which has been virtually ruled out (Halpern & Filippenko 1992). Since the binary model offers no explanation for the absence of Lyα in Arp 102B, we continue to regard it as inapplicable.

Additional models for double-peaked emission lines in AGNs fall into three classes. The first involves jets or biconical radial flows and is purely kinematic. The velocity field and emissivity are adjusted essentially arbitrarily to reproduce the observed line profiles (e.g., Zheng, Binette, & Sulentic 1990; Sulentic et al. 1995). The second class of model is a time-dependent generalization of the first, in which a variable continuum source photoionizing a system of outflowing clouds produces double-peaked profiles with time-varying asymmetries (Robinson, Pérez, & Binette 1990; Pérez, Robinson, & de la Fuente 1992) resembling those that are sometimes observed. The third class of alternative models involves an anisotropic ionizing continuum. As proposed by Wanders et al. (1995), a pair of collimated ionizing beams illuminating a spherically symmetric distribution of clouds on randomly inclined circular orbits can produce double-peaked emission lines if the beams are oriented at large angles from the line of sight.

The main advantage of radial outflow models is their ability to reproduce line *profiles* that are not fitted by simple disk models, albeit in a manner which is ad hoc and not necessarily rooted in a dynamical model. As such, they are difficult to test and difficult to rule out. However, these models are not (yet) equipped to deal with the peculiar line *ratios* which the UV spectrum of Arp 102B reveals. The absence of double-peaked Lyα may prove to be their most severe challenge. Similarly, the "searchlight" model of Wanders et al. (1995) assumes otherwise standard photoionization theory of broad-line region clouds, so does not address the absence of Lyα in the displaced peaks. The suppression of Lyα might be accomplished by dust mixed internally with the emitting gas, but we argued in § 4.1 that extinction by dust is not likely to be the sole cause. Instead, large optical depth, high density, and small velocity gradient along the line of sight to the observer are probably required. All of these conditions are naturally fulfilled in an accretion disk, in which the high density is maintained by material with circular velocity much larger than its radial velocity. Velocity gradients along the line of sight through a disk are minimal.

Radial flows require a much larger mass flux than does an accretion disk to maintain the same density and velocity. Assume that a photoionized radial flow which we hypothesize to emit the Balmer lines needs to subtend a solid angle similar to that of the accretion disk. Mass continuity then prevents the density of such a flow from exceeding of order v_r/v_ϕ times the density of the disk which presumably feeds it, where v_r and v_ϕ are the radial and azimuthal velocities in the disk. In the standard thin disk, $v_r/v_\phi \simeq \alpha(h/r)^2$, where α is the viscosity parameter, $h(r)$ is the height, and r is the radial coordinate. As long as $(\dot{M}/\dot{M}_{\rm Edd})\alpha^{-2} \leq 50$, a disk in which $h \simeq r$ is an optically thin ion-supported torus (Rees et al. 1982), and not an atomic gas.

Even if this material were made to flow out and cool to $\sim 10^4$ K, it could not both subtend a large solid angle (e.g., a spherical shell) and maintain the column density necessary to suppress Lyα. Furthermore, to produce the large line widths observed in the double peaks, a collimated radial flow needs a velocity gradient along the line of sight, which would further promote the escape of Lyα. Although detailed calculations have not yet been made, we expect that the striking absence of Lyα will be difficult to accommodate in radial flow models for double-peaked Balmer lines.

5. ABSORPTION LINES

5.1. *Line Identifications*

The G270H spectrum contains a plethora of absorption lines, as shown in Figure 4. Several of these are superposed on the double-peaked Mg II emission line. A minority of the

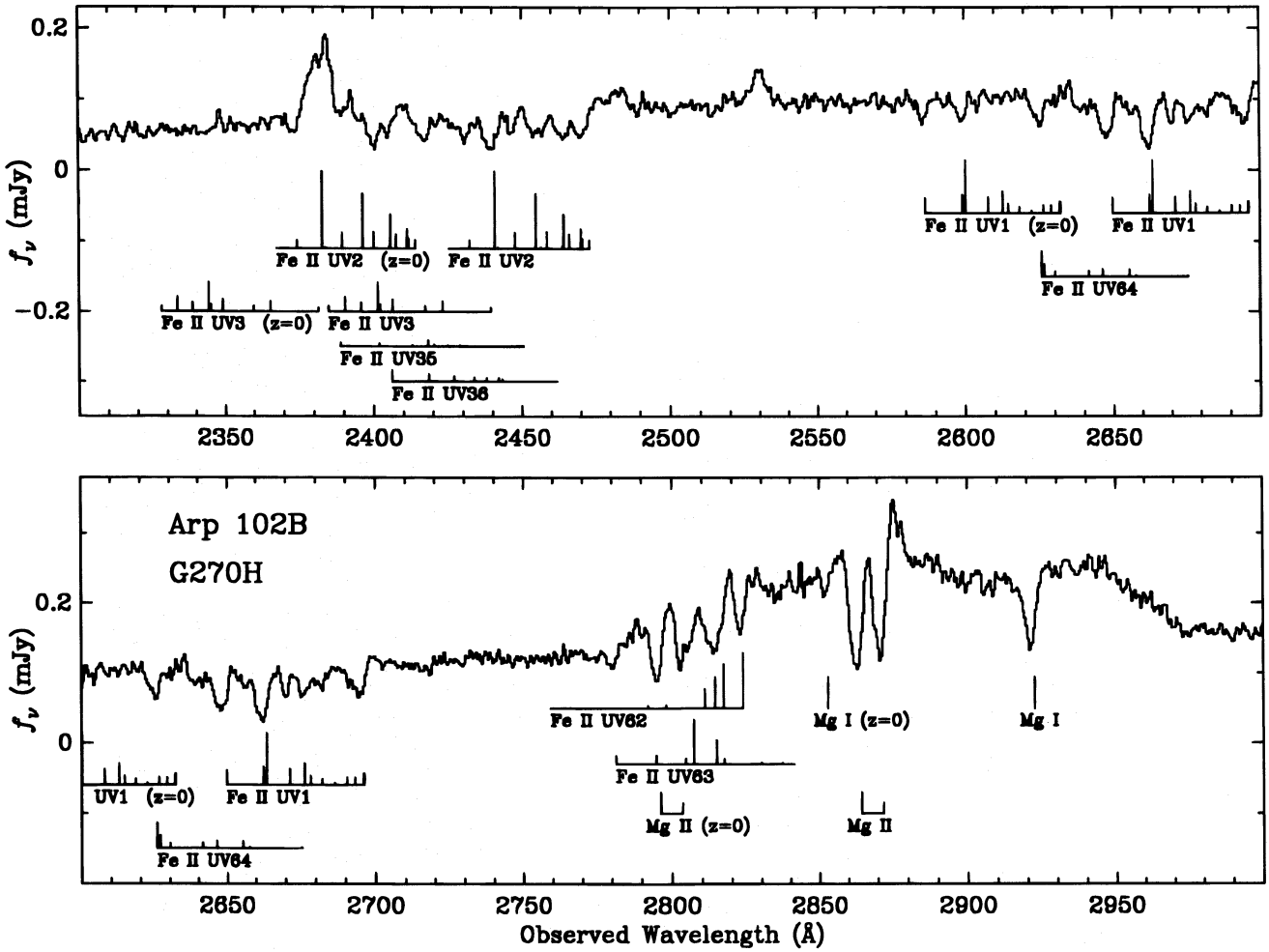

FIG. 4.—The G270H spectrum of Arp 102B, with identified absorption lines of Mg I, Mg II, and Fe II multiplets. The spectra are smoothed with a triangular function half as wide as the resolution. Galactic resonance lines at $z = 0$ are marked, and all intrinsic absorption is marked at the systemic (narrow-line) redshift $z = 0.02438$. The height of each tick mark is proportional to its gf-value. Wavelengths and gf-values of Fe II were taken from Fawcett (1987).

absorption lines can be identified with prominent interstellar features in our Galaxy ($z = 0$), namely Mg I λ2852.1, Mg II $\lambda\lambda$2795.5, 2802.7, Fe II λ2599.4, and Fe II λ2585.9. The same transitions are present in greater strength at the systemic redshift of Arp 102B. We adopt the narrow emission-line redshift, $z = 0.02438$, as the systemic value. Identifying tick marks in Figure 4 are placed at this redshift. Also present at the systemic redshift are absorption in Lyα and C IV, which are often seen in Seyfert galaxies. The remaining absorption lines comprise a large number of Fe II transitions at the Redshift of Arp 102B that are *not* observed in the interstellar medium of our own Galaxy. As described below, we interpret these intrinsic absorption lines as constituting a rare type of associated absorption system similar to that seen in two broad absorption-line quasars (BALQSOs).

Normally, only transitions arising from the Fe II ground-state term (a^6D) are observed in QSO absorption-line systems (e.g., Barthel, Tytler, & Thomson 1990; Junkkarinen, Hewitt, & Burbidge 1991) and in the interstellar medium of the Galaxy. This is true of all the interstellar Fe II absorption lines seen in the spectra of SN 1987A (Blades et al. 1988) and the bright QSOs 3C 273, H1821+643, and Mrk 205 (Bahcall et al. 1991, 1992a, b; Morris et al. 1991). The prominent Fe II ground-state transitions are members of multiplets UV1, UV2, and UV3. The only Fe II lines that we can identify with certainty at $z = 0$ are λ2599.4, λ2598.4 and λ2585.9 of multiplet UV1. Possibly present at $z = 0$ are the lines at 2382.0, 2395.6, and 2404.9 Å of multiplet UV2, but these are blended with other Fe II lines at the redshift of the AGN and with the C II] λ2326 emission line.

In contrast to the paucity of Galactic absorption lines, we have identified at the redshift of Arp 102B contributions from eight different multiplets of Fe II arising from the three lowest terms (a^6D, a^4F, and a^4D). In addition to the prominent ground state transitions from a^6D, we see multiplets UV62, UV63, and UV64 arising from the metastable a^4D term which lies 0.99–1.10 eV above the ground state. These are responsible for obliterating a significant fraction of the flux in the blueshifted peak of the broad Mg II emission line and are partly blended with the Mg II doublet at $z = 0$. (The absorption-line wavelengths do not support an alternative identification of any of the absorption on the blue side of the Mg II emission with outflowing Mg II doublets.) Contributions from Fe II multiplets UV35 and UV36 arising from the metastable a^4F term 0.23–0.39 eV above the ground state also appear to be necessary in order to account for the strength of an absorption line at an observed wavelength of 2417 Å. This could be a blend of Fe II $\lambda\lambda$2360.0, 2360.3 with a line at 2359.1 Å from multiplet UV3, all at $z = 0.02438$.

It is difficult to identify all the individual lines contributing to the absorption blends, particularly because many of their oscillator strengths are uncertain by a factor of 2 or more. The heights of the tick marks in Figure 4 are proportional to the theoretical *gf*-values as given by Fawcett (1987), although several observational and laboratory measurements have been made recently (Shull, Van Steenberg, & Seab 1983; Ekberg & Feldman 1993; Bergeson, Mullman, & Lawler 1994) which should be more accurate. Despite the uncertain line strengths, it is clear that the wide forests of lines and breaks in the G270H spectrum are due largely to overlapping Fe II multiplets at or near the systemic redshift.

5.2. *A Metastable Associated Absorber*

The strong absorption lines from excited levels of Fe II in Arp 102B are incompatible with a diffuse interstellar medium there, and therefore constitute an "associated absorber"—namely, warm gas associated with the active nucleus in some way that remains to be understood. Somewhat unusual properties of this system are (1) the low ionization level of the species present and (2) the fact that the absorption lines are very close to the systemic velocity. But the most unusual feature is (3) the presence of absorption from metastable levels with excitation potentials of up to 1.1 eV.

The subclass of Mg II (low-ionization) BALQSOs (e.g., Voit, Weymann, & Korista 1993) offers a precedent for the low ionization level. As for the small velocity of the absorption lines, Seyfert galaxies often exhibit variable UV absorption lines which are blueshifted by 1000 km s^{-1} or less from the emission-line velocity. These have been interpreted as low-power analogs of the BALQSOs (e.g., Kolman et al. 1993), of which Arp 102B may be the weakest example yet found. It is characteristic of many of these absorption-line profiles in Seyferts that the red edge is steeper than the blue edge, as though the absorbing clouds were gradually accelerated from a fixed starting velocity. Several of the absorption lines in Arp 102B, such as Mg I, Mg II, and Fe II λ2755.7, are well enough isolated to see that they are broader than the resolution of $\sim$200 km s^{-1}. Careful inspection of their profiles reveals that they are asymmetric in the aforementioned sense, and that their lowest points are possibly blueshifted from the emission-line velocity by $\sim$160 km s^{-1}. Since the absorption-line profiles are not well resolved, we can derive only lower limits to the column densities from their optical depths, using the method of Junkkarinen, Burbidge, & Smith (1983),

$$N \geq \left(\frac{v_0 mc}{\pi e^2 f}\right) \int \tau \, d \ln \lambda \, , \qquad (1)$$

where v_0 is the rest frequency and f is the oscillator strength. For Mg I, we derive $N_{\rm Mg^0} > 2 \times 10^{13}$ cm^{-2}, while for Mg II, a crude estimate obtained from the doublet by connecting the highest points on either side with a linear continuum yields $N_{\rm Mg^+} > 2 \times 10^{14}$ cm^{-2}. Assuming a cosmic abundance of Mg, these values correspond to much smaller effective hydrogen column densities than are usually discussed with regard to the emission-line regions.

By far the most unusual characteristic of this absorption spectrum is the presence of metastable levels with excitation potentials of up to 1.1 eV. This phenomenon is not observed in ordinary Seyfert or radio galaxies, and not at the systemic velocity of any appropriately observed AGN. The only exception of which we are aware is NGC 4151, in which an absorption line of C III] λ1176 has been detected (Kriss et al. 1995), arising from the metastable level 6.50 eV above the ground state.

Among all QSO absorption-line systems, such high excitation has definitely been seen to our knowledge in only two objects, Q0059−2735 (Hazard et al. 1987; Wampler, Chugai, & Petitjean 1995), and the luminous infrared Seyfert galaxy Mrk 231 (Boroson et al. 1991; Smith et al. 1995). The latter has multiple absorption-line systems blueshifted by 4600–8200 km s^{-1} from the emission-line velocity (Boroson et al. 1991; Forster, Rich, & McCarthy 1995). In addition to the Na I D resonance line, He I λ3889 and

He I λ3188 lines are seen in absorption in Mrk 231, as are Fe II multiplets UV1, UV2, UV63 (Smith et al. 1995). We infer the probable presence of UV62 as well in the Smith et al. spectrum of Mrk 231.

Q0059−2735 at $z = 1.595$ is a BALQSO in which a plethora of *narrow* ($b \lesssim 20$ km s^{-1}) absorption lines from excited levels of low-ionization species are also seen. Wampler et al. (1995) have interpreted the narrow lines as arising from low-ionization condensations in a hotter BAL flow. The excitation level of the narrow Fe II absorption spectrum in this QSO is very similar to that of Arp 102B. Weaker lines from even higher levels of Fe II are seen in the high-resolution spectrum of the QSO, but we would not be able to detect such weak lines in our spectrum of Arp 102B if they were present. The excitation temperature of the metastable Fe II levels in both of these objects is likely to be $\sim 10^4$ K, which, if collisionally excited, would require electron density $n_e > 10^6$ cm^{-3} (Wampler et al. 1995). Alternatively or additionally, radiative pumping could be important.

5.3. *Other Possibilities*

Although the evidence points strongly toward an associated absorber model, we briefly considered an alternative explanation, namely, that the absorption lines are actually from the starlight of the underlying galaxy. This possibility cannot be dismissed immediately because (1) the visible spectrum is in fact dominated by starlight, (2) the UV absorption lines present are common to a wide range of stellar types from late A through early K (Fanelli et al. 1992), and (3) the redshift and "dispersion" of the lines are not grossly discrepant from the stellar continuum observed in the visible. Nevertheless, we feel that starlight is a negligible contributor to the absorption lines because (1) the spectral decomposition of the continuum into a power law plus a normal elliptical galaxy (see § 2.3) allows very little starlight in the near UV in a 0.″9 aperture, (2) the UV spectrum of Arp 102B is significantly different from that of normal elliptical galaxies and the bulges of spirals such as M31, and especially, (3) the stronger absorption lines that are superposed on the Mg II emission line are slightly deeper than the continuum, so they must cover some of the emission-line region as well. In normal galaxies, the absorption spectrum longward of 2800 Å is dominated by broad blends of Fe I which are not present in Arp 102B. An elliptical galaxy spectrum is apparently dominated by K giants even in the near-UV, whereas the UV continuum of Arp 102B, if due to starlight, would have to comprise hotter stars, none of which provides an adequate match to the overall spectrum. To make this assessment, we examined the *IUE* libary of stellar spectra (Fanelli et al. 1992), *IUE* spectra of normal and star-forming galaxies (Bruzual, Peimbert, & Torres-Peimbert 1982; Welch 1982; Kinney et al. 1993), and the aforementioned FOS spectra of the elliptical galaxies NGC 1399 and NGC 3610.

Since we have invoked an accretion disk for the origin of the low-ionization emission lines, we might consider the possibility that the absorption lines also arise in the disk atmosphere, but at a much larger radius. But the covering of the Mg II emission line by the absorption line rules against this hypothesis, just as it did for a stellar origin. However, it is plausible that the absorbing gas originates in a low-velocity wind from the accretion disk (e.g., Murray et al. 1995). Perhaps the same geometry that allows the ionizing continuum to power emission lines from the disk is especially favorable for the generation of a wind.

In summary, we consider that the UV spectrum of Arp 102B is best described as a nonstellar continuum whose absorption features can be accounted for entirely by warm gas associated with the active nucleus. The absence of detectable absorption lines in the visible spectrum (e.g., Na I D) is perhaps attributable to the strength of the stellar continuum at that wavelength, which at this moderate spectral resolution masks any additional gaseous absorption features. We leave detailed modeling of the associated absorber, such as a comparison of collisional versus radiative excitation, for a later study. Since the depth of the Mg II absorption line requires it to cover the entire continuum source as well as at least part of the broad-line region, an origin in the narrow-line region may be possible. This would be of interest in view of the low ionization level of the narrow emission lines of Arp 102B (Table 3; see also Stauffer et al. 1983), which is in fact a low-ionization nuclear emission-line region (LINER; Heckman 1980).

6. CONCLUSIONS AND SPECULATIONS

We regard the agreement of its double-peaked line strengths with the accretion-disk model, and the clean separation of its additional "ordinary" broad-line component in both the UV and optical data, as compelling justification for the consideration of separate emission-line sources in Arp 102B, and by extension, in similar objects as well. It is no longer reasonable to hope that a single model will account for all "broad lines," especially not among the unusual class of double-peaked emitters identified by Eracleous & Halpern (1994). The conspicuous absence of Lyα from the double-peaked family of lines in Arp 102B is especially worrisome for scenarios such as jets or biconical outflows, since the conditions required for line destruction, namely, high-density, large optical thickness, and small line-of-sight velocity gradient, are difficult to achieve without expelling more mass than is accreted through the disk itself. The accretion disk achieves its thickness by circulating the same material many times, which radial outflows by definition do not.

Additional evidence that single-peaked and double-peaked emission lines require independent sources comes from the emergence of a double-peaked Balmer line component in the broad-line radio galaxy Pic A while its ordinary broad line remained constant (Halpern & Eracleous 1994). Pic A, however, is not particularly supportive of an accretion-disk origin for its displaced Balmer lines because its peaks are too well separated, with little or no emission at zero radial velocity (Halpern & Eracleous 1994; Sulentic et al. 1995). In addition, the displaced peaks in Pic A are variable in intensity, but do not vary in phase with each other.

The fact that double-peaked emitters are almost exclusively found among radio galaxies or LINERs (Arp 102B is both) is undoubtedly an important clue to their nature that has yet to be fully exploited (Halpern & Eracleous 1994). Study of line-profile variability is often mentioned as the best hope of understanding AGN emission lines. In addition to posing a challenge to accretion-disk models, observed variability has inspired a number of physically motivated proposals involving spiral waves in disks (Chakrabarti & Wiita 1994), hot spots in disks (Zheng et al. 1991), tidal disruption of stars (Storchi-Bergmann et al. 1995), and elliptical disks (Eracleous et al. 1995). The line-

profile variability of Arp 102B is relatively modest compared to some of the other objects discussed in these references, so we should certainly not feel that by studying Arp 102B we have learned all that we need to know about the double-peaked emitters.

Anticipating how this investigation may be extended to other objects, it is first important to determine how widespread is the absence of double-peaked Lyα among broad-line radio galaxies that have disklike Balmer lines. We suspect that this might be a general phenomenon, because we do not know of any clearly double-peaked Lyα lines in the *IUE* spectra of radio galaxies, or in any ground-based spectra of high-redshift quasars. Approved *HST* observations of additional double-peaked emitters will soon address this question.

Another use of these data concerns the properties of the continuum. By combining the FOS and ground-based optical spectra with soft and hard X-ray data, it will be possible to test whether the ionizing continua of double-peaked emitters differ from those of ordinary Seyfert galaxies. The steep power laws that fit the optical and FOS spectra ($\alpha = 2.1$–2.4, see § 2.3) indicate an absence of a UV bump. As speculated for Arp 102B, the lack of a UV bump may constitute both the evidence that the ionizing continuum is hard, and the clue that the outer disk is being illuminated by that continuum. A dilute, hard continuum may be responsible for the association of double-peaked emitters with LINERs, and perhaps in some way for the peculiar associated absorber that made its serendipitous appearance here for the first time. We will pursue these additional investigations of Arp 102B and will incorporate additional objects with forthcoming FOS spectra.

This work was supported by STScI grant GO-5428-93A. The observations were carried out at the Space Telescope Science Institute, which is operated by the Association of Universities for Research in Astronomy, Inc., under NASA contract NAS 5-26555. We thank Henry Ferguson for allowing us to make use of his FOS spectra of elliptical galaxies, and Gerard Kriss for advice about background contamination in FOS spectra. We are grateful for the assistance of Aaron J. Barth during acquisition and reduction of the Lick optical spectra. This paper is contribution 581 of the Columbia Astrophysics Laboratory.

REFERENCES

Antonucci, R., Hurt, T., & Agol, E. 1996, ApJ, 456, L25
Ayres, T. R. 1993, Instr. Sci. Rep. CAL/FOS-115
Bahcall, J. N., Jannuzi, B. T., Schneider, D. P., Hartig, G. F., Bohlin, R., & Junkkarinen, V. 1991, ApJ, 377, L5
Bahcall, J. N., Jannuzi B. T., Schneider, D. P., Hartig, G. F., & Green, R. F. 1992a, ApJ, 397, 68
Bahcall, J. N., Jannuzi, B. T., Schneider, D. P., Hartig, G. F., & Jenkins, E. B. 1992b, ApJ, 398, 495
Barthel, P. D., Tytler, D. R., & Thomson, B. 1990, AJ, 82, 339
Bergeson, S. D., Mullman, K. L., & Lawler, J. E. 1994, ApJ, 435, L157
Biermann, P., Kronberg, P. P., Preuss, E., Schilizzi, R. T., & Shaffer, D. B. 1981, ApJ, 250, L49
Blades, J. C., Wheatley, J. M., Panagia, N., Grewing, M., Pettini, M., & Wamsteker, W. 1988, ApJ, 334, 308
Boroson, T. A., Meyers, K. A., & Morris, S. L. 1991, ApJ, 370, L19
Bruzual, G., Piembert, M., & Torres-Peimbert, S. 1982, ApJ, 260, 495
Chakrabarti, S., & Wiita, P. J. 1994, ApJ, 434, 518
Chen, K., & Halpern, J. P. 1989, ApJ, 344, 115
———. 1990, ApJ, 345, L1
Chen, K., Halpern, J. P., & Filippenko, A. V. 1989, ApJ, 339, 742
Collin-Souffrin, S. 1987, A&A, 179, 60
Colin-Souffrin, S., & Dumont, A. M. 1990, A&A, 229, 292
Dahlem, M., & Koratkar, A. 1994, Instr. Sci. Rep. CAL/FOS-131
Dumont, A. M., & Collin-Souffrin, S. 1990a, A&A, 229, 302
———. 1990b, A&A, 229, 313
———. 1990c, A&AS, 83, 71
Ekberg, J. O., & Feldman, U. 1993, ApJS, 86, 611
Eracleous, M., & Halpern, J. P. 1993, ApJ, 409, 584
———. 1994, ApJS, 90, 1
Eracleous, M., Livio, M., Halpern, J. P., & Storchi-Bergmann, T. 1995, ApJ, 438, 610
Fanelli, M. N., O'Connell, R. W., Burstein, D., & Wu, C.-C. 1992, ApJS, 82, 197
Fawcett, B. C. 1987, Atomic Data Nucl. Data Tables, 37, 333
Filippenko, A. V., & Sargent, W. L. W. 1988, ApJ, 324, 134
Forster, K., Rich, R. M., & McCarthy, J. K. 1995, ApJ, 450, 74
Gaskell, C. M. 1983, in Quasars and Gravitational Lenses, Proc. 24th Liège Astrophysical Colloq. (Liège: Institut d'Astrophysique, Univ. Liège), 473
Halpern, J. P. 1990, ApJ, 365, L51
Halpern, J. P., & Eracleous, M. 1994, ApJ, 433, L17
Halpern, J. P., & Filippenko, A. V. 1988, Nature, 331, 46
———. 1992, in AIP Conf. Proc. No. 254, Testing the AGN Paradigm, ed. S. S. Holt, S. G. Neff, & C. M. Urry (New York: AIP), 57
Hazard, C., McMahon, R. G., Webb, J. K., & Morton, D. C. 1987, ApJ, 323, 263
Heckman, T. M. 1980, A&A, 87, 152
Junkkarinen, V. T., Burbidge, E. M., & Smith, H. E. 1983, ApJ, 265, 51
Junkkarinen, V., Hewitt, A., & Burbidge, G. 1991, ApJS, 77, 203
Kinney, A. L., & Bohlin, R. C. 1993, Instr. Sci. Rep. CAL/FOS-103
Kinney, A. L., Bohlin, R. C., Calzetti, D., Panagia, N., & Wyse, R. F. G. 1993, ApJS, 86, 5
Kolman, M., Halpern, J. P., Martin, C., Awaki, H., & Koyama, K. 1993, ApJ, 403, 592
Koratkar, A., & Evans, I. 1995, Instr. Sci. Rep. CAL/FOS-142
Kriss, G. A., Blair, W. P., & Davidsen, A. F. 1991a, Instr. Sci. Rep. CAL/FOS-060
———. 1991b, Instr. Sci. Rep. CAL/FOS-067
Kriss, G. A., Davidsen, A. F., Zheng, W., Kruk, J. W., & Espey, B. R. 1995, ApJ, 454, L7
Miller, J. S., & Peterson, B. M. 1990, ApJ, 361, 98
Miller, J. S., & Stone, R. P. S. 1993, Lick Obs. Tech. Rep., No. 66
Morris, S. L., Weymann, R. J., Savage, B. D., & Gilliland, R. L. 1991, ApJ, 377, L21
Murray, N., Chiang, J., Grossman, S. A., & Voit, G. M. 1995, ApJ, 451, 498
Netzer, H., & Laor, A. 1993, ApJ, 404, L51
Pérez, E., Robinson, A., & de la Fuente, L. 1992, MNRAS, 255, 502
Puschell, J. J., Moore, R., Cohen, R. D., Owen, F. N., & Phillips, A. C. 1986, AJ, 91, 751
Rees, M. J., Begelman, M. C., Blandford, R. D., & Phinney, E. S. 1982, Nature, 295, 17
Rees, M. J., Netzer, H., & Ferland, G. J. 1989, ApJ, 347, 640
Robinson, A., Pérez, E., & Binette, L. 1990, MNRAS, 246, 349
Rokaki, E., Boisson, C., & Collin-Souffrin, S. 1992, A&A, 253, 57
Rosa, M. R. 1993, Instr. Sci. Rep. CAL/FOS-114
———. 1994, Instr. Sci. Rep. CAL/FOS-127
Shields, J. C., & Ferland, G. J. 1993, ApJ, 402, 425
Shull, J. M., Van Steenberg, M., & Seab, C. G. 1983, ApJ, 271, 408
Smith, P. S., Schmidt, G. D., Allen, R. G., & Angel, J. R. P. 1995, ApJ, 444, 146
Stark, A. A., Gammie, C. F., Wilson, R. W., Bally, J., Linke, R. A., Heiles, C., & Hurwitz, M. 1992, ApJS, 79, 77
Stauffer, J., Schild, R., & Keel, W. C. 1983, ApJ, 270, 465
Storchi-Bergmann, T., Eracleous, M., Livio, M., Wilson, A. S., Filippenko, A. V., & Halpern, J. P. 1995, ApJ, 443, 617
Sulentic, J. W., Marziani, P., Zwitter, T., & Calvani, M. 1995, ApJ, 438, L1
Veilleux, S., & Zheng, W. 1991, ApJ, 377, 89
Voit, G. M., Weymann, R. J., & Korista, K. T. 1993, ApJ, 413, 95
Wampler, E. J., Chugai, N. N., & Petitjean, P. 1995, ApJ, 443, 586
Wanders, I., et al. 1995, ApJ, 453, L87
Welch, G. A. 1982, ApJ, 259, 77
Yee, H. K. C., & Oke, J. B. 1978, ApJ, 226, 753
Zheng, W., Binette, L., & Sulentic, J. W. 1990, ApJ, 365, 115
Zheng, W., Veilleux, S., & Grandi, S. A. 1991, ApJ, 381